

2022

***PHIP* Variants Associated with Chung–jansen Syndrome Disrupt Replication Fork Stability and Genome Integrity**

Neysha Tirado-Class
University of South Florida

Caitlin Hathaway
University of South Florida

Wendy K. Chung
Columbia University

Huzefa Dungrawala
University of South Florida, hdungrawala@usf.edu

Follow this and additional works at: https://digitalcommons.usf.edu/bcm_facpub

 Part of the [Cell Biology Commons](#), [Microbiology Commons](#), and the [Molecular Biology Commons](#)

Scholar Commons Citation

Tirado-Class, Neysha; Hathaway, Caitlin; Chung, Wendy K.; and Dungrawala, Huzefa, "*PHIP* Variants Associated with Chung–jansen Syndrome Disrupt Replication Fork Stability and Genome Integrity" (2022). *Molecular Biosciences Faculty Publications*. 99.
https://digitalcommons.usf.edu/bcm_facpub/99

This Article is brought to you for free and open access by the Molecular Biosciences at Digital Commons @ University of South Florida. It has been accepted for inclusion in Molecular Biosciences Faculty Publications by an authorized administrator of Digital Commons @ University of South Florida. For more information, please contact digitalcommons@usf.edu.



PHIP variants associated with Chung–Jansen syndrome disrupt replication fork stability and genome integrity

Neysha Tirado-Class,¹ Caitlin Hathaway,¹ Wendy K. Chung,^{2,3} and Huzefa Dungalwala¹

¹Department of Cell Biology, Microbiology and Molecular Biology, University of South Florida, Tampa, Florida 33620, USA; ²Department of Pediatrics, ³Department of Medicine, Columbia University, New York, New York 10032, USA

Abstract Chung–Jansen syndrome (CJS) is a rare, autosomal dominant disorder characterized by developmental delay, intellectual disability/cognitive impairment, behavioral challenges, obesity, and dysmorphic features. CJS is associated with heterozygous variants in *PHIP* (Pleckstrin-Homology Interacting Protein), a gene that encodes one of several substrate receptors for Cullin4-RING (CRL4) E3 ubiquitin ligase complex. Full-length *PHIP*, also called DCAF14, was recently identified to function as a replication stress response protein. Herein, we report the identification of two *PHIP* missense variants identified by exome sequencing in unrelated individuals with CJS. The variants p.D488V and p.E963G occur in different functional elements of DCAF14-WD40 repeat domain and pleckstrin homology-binding region (PBR), respectively. Using DNA fiber assays, we reveal that cells expressing either variant exhibit defective replication fork progression in conditions of replication stress. Furthermore, unlike wild-type DCAF14, both variants fail to accomplish DNA replication after exposure to genotoxic stress indicating a critical role of DCAF14 in protecting stalled replication forks. Thus, we have identified replication defects associated with CJS variants and predict replication-associated genome instability with CJS syndrome.

Corresponding author:
hdungalwala@usf.edu

© 2022 Tirado-Class et al. This article is distributed under the terms of the Creative Commons Attribution-NonCommercial License, which permits reuse and redistribution, except for commercial purposes, provided that the original author and source are credited.

Ontology terms: 2-3 toe syndactyly; abdominal obesity; generalized neonatal hypotonia; intellectual disability; moderate; mild global developmental delay

Published by Cold Spring Harbor Laboratory Press

doi:10.1101/mcs.a006212

[Supplemental material is available for this article.]

INTRODUCTION

Macromolecular machines called replisomes duplicate both genetic and epigenetic information during each S phase of the cell cycle. DNA replication is inherently challenged by various endogenous and exogenous obstacles that stall ongoing replication forks, causing replication stress (Zeman and Cimprich 2014). Sources of replication stress include collisions with ongoing transcription machinery, DNA helix distorting lesions, and difficult to replicate genomic regions. Stalled replication forks must be stabilized and protected from fork collapse to ensure accurate and efficient duplication of the genome (Saldivar et al. 2017). Multiple pathways promote replication fork stability to safeguard genome integrity, and many function in the ATR (ataxia telangiectasia mutated and rad3 related) checkpoint signaling cascade. Protein components in this pathway stabilize forks, protect newly synthesized DNA, and induce cell cycle arrest to ensure damage is repaired and forks restarted in a timely manner for ensuing mitosis.

Defects in DNA replication and replication stress response cause syndromes often characterized by developmental delay, intellectual disabilities, and increased cancer

predisposition (Bellelli and Boulton 2021). Loss-of-function variants in proteins that promote prereplication complex formation, origin activation, and replication frequently cause microcephalic dwarfism. For example, hypomorphic variants in the prerecognition complex cause Meier–Gorlin syndrome (MGORS) because of perturbed replication dynamics (Ladha 2011). Defects in ATR and the obligatory ATR-binding protein ATRIP cause Seckel syndrome (SS) because replication stress response is compromised in SS patients (O’Driscoll et al. 2003; Ogi et al. 2012; Mokrani-Benhelli et al. 2013). There is a group of genetic syndromes due to defects in accurate processing and repair of stalled replication forks that include Werner syndrome (WRN), Bloom syndrome (BLM), and Schimke immune-osseous dysplasia disorder (SIOD) characterized by severe developmental abnormalities and accelerated aging (Boerkoel et al. 2002; Cunliffe et al. 2017; Oshima et al. 2017). Thus, there are human genetic disorders directly linked to DNA replication and stress response that highlight the need and opportunities to address disease characteristics in individuals affected by faulty DNA replication.

Chung–Jansen syndrome (CJS) is an autosomal dominant disorder associated with Developmental Delay, Intellectual Disability, Obesity, and Dysmorphism (DIDOD) (OMIM #617991). The syndrome is caused by de novo or rarely inherited largely predicted loss of function variants in pleckstrin-homology interacting protein (*PHIP*), a gene on Chromosome 6q14.1. De novo variants in *PHIP* were first identified by exome sequencing in individuals with intellectual disability (de Ligt et al. 2012). Multiple follow-up studies later identified more than 25 individuals with clinical phenotypes of CJS harboring heterozygous de novo variants predicted to disrupt *PHIP* function (Webster et al. 2016; Jansen et al. 2018; Craddock et al. 2019). A smaller number of de novo missense variants predicted to be deleterious have also been identified in individuals with features of CJS (Webster et al. 2016; Jansen et al. 2018; Craddock et al. 2019). *PHIP* codes for three distinct isoforms in humans: an 1821-amino-acid-long full-length protein called DDB1- and CUL4-associated factor 14 (DCAF14), a 902-amino-acid protein lacking the amino terminus named PHIP (Farhang-Fallah et al. 2000), and an 1019-amino-acid protein lacking the carboxyl terminus called NDRP (Kato et al. 2000). Previous studies have predicted that disruptions in DCAF14 are the primary driver of CJS phenotypes (Jansen et al. 2018). DCAF14 functions as a substrate receptor for a highly conserved Cullin4-DDB1 (CRL4) E3 ubiquitin ligase family that functions as critical mediators of genome stability and cellular survival (Jin et al. 2006). DCAF14 has a WD40-repeat domain, two bromodomains, and pleckstrin-homology interacting domain (PBR). The PBR region is responsible for mediating the interaction of PHIP with the pleckstrin homology domain of insulin receptor substrate-1 (Farhang-Fallah et al. 2000). Although bromodomains recognize acetylated lysine residues on histones and nonhistone proteins (Fujisawa and Filippakopoulos 2017), the WD40-repeat domains in multiple DCAFs contain highly conserved WDXR motifs responsible for DCAF interaction with the adaptor protein DDB1 of CRL4 complexes (Jin et al. 2006).

DCAF14 promotes pancreatic β -cell mitogenesis (Podcheko et al. 2007), regulates metaphase-to-anaphase transition (Jang et al. 2020), and is a biomarker for metastatic melanoma (De Semir et al. 2012). Additionally, DCAF14 also functions in regulating key aspects of DNA replication. DCAF14/RepID regulates origin initiation events by recruiting CUL4 to chromatin (Jang et al. 2018). DCAF14 is also recruited to stalled replication forks and stabilizes newly synthesized DNA to prevent replication fork collapse (Townsend et al. 2021). However, the molecular mechanism of CJS syndrome is currently not established. Thus, we sought to determine whether *PHIP* variants disrupt the replication stress response function of DCAF14 at stalled replication forks.

In this study, we describe the identification and characterization of two *PHIP* variants in individuals with CJS. Both missense variants, p.D488V and p.E963G, are in known functional domains of DCAF14. Using site-directed mutagenesis for functional analyses, we demonstrate that the disease variants are incapable of supporting DNA replication in conditions

of replication stress. Furthermore, p.D488V causes collapse of stalled replication forks into double-strand breaks (DSBs). Importantly, both disease variants induce 53BP1 bodies in the subsequent G₁ phase after exposure to genotoxic stress, indicating compromised genome stability. Thus, our study associates *PHIP* loss-of-function CJS variants with defective DCAF14 function in stabilizing stalled replication forks.

RESULTS

Identification of *PHIP* Variants

Both participants had exome sequencing and were found to have heterozygous de novo *PHIP* variants (Table 1). The p.E963G variant is also reported in another patient (#360936) in DECIPHER. We compiled a list of all published *PHIP* variants to compare the mode of inheritance, potential deleteriousness scores from prediction algorithms, and location in a known functional domain (Table 2). More than 60% of the variants were confirmed as de novo. Both *PHIP* de novo variants, p.D488V and p.E963G, exhibit high score annotations for deleteriousness by PolyPhen-2, PROVEAN, and Mutation Taster. Additionally, amino acid residues 488 and 963 are located in known functional domains of DCAF14, the WD40-repeat domain, and the PBR domain, respectively (Fig. 1A).

Clinical Presentation of Features

PHIP020 is a 4.8-yr-old female with a de novo c. 2888A > G p.E963G *PHIP* variant detected on trio exome sequencing. She was born at 40 wk of gestation with a birth weight of 2.75 kg ($Z = -1.4$) and length of 49 cm ($Z = -0.2$). She was briefly hypoglycemic as a newborn. She had feeding difficulty and was irritable as an infant. As she developed she was hypotonic and had gross and fine motor delay, dyspraxia, excessive clumsiness and difficulty with coordination, and speech delay. Medically she had orthopedic issues: hip dysplasia and scoliosis, and her hip dysplasia required surgery at 1 yr of age. She had vision issues including myopia, strabismus, and difficulty with depth perception. She had gastrointestinal issues including gastroesophageal reflux disease, irritable bowel and chronic constipation, and an umbilical hernia. Her current weight is 17 kg ($Z = -0.5$) and height is 1.04 m ($Z = -0.8$). She has unilateral 2-3 toe syndactyly. She fatigues easily. She has neurobehavioral issues including anxiety, attention disorder, mood swings, sensory processing disorder, sensitivity to sound, and autism. Her Vineland adaptive behavioral scale composite score was 77 (mean 100 and standard deviation of 15), communication subscore of 76, daily living skills subscore of 81, socialization subscore of 81, and motor skills subscore of 78.

PHIP023 is a 4-yr-old female with a c.1463 A > T p.D488V *PHIP* variant detected on trio exome sequencing. She was born at 38 wk of gestation with a birth weight of 2.9 kg ($Z = -1$) and length of 48.5 cm ($Z = -0.4$) and had no neonatal complications. She has medically been largely healthy. She has vision issues including myopia and astigmatism. She has a history of chronic constipation. Her current weight is 14 kg ($Z = -1.1$) and her height is 94 cm ($Z = -1.6$).

Table 1. Variants identified in this study

Gene	Chromosome	HGVS DNA reference	HGVS protein reference	Variant type	Predicted effect	dbSNP/dbVar ID	Genotype
<i>PHIP</i>	6q14.1	c.1463A > T	p.D488V	Missense	Loss of function	None	Heterozygous
<i>PHIP</i>	6q14.1	c.2888A > G	p.E963G	Missense	Loss of function	None	Heterozygous

(HGVS) Human Genome Variation Society, (dbSNP) Database for Short Genetic Variations, (dbVar) Database for Genomic Structural Variation.

Table 2. List of published PHIP variants

Variant ^a	Inheritance	PolyPhen-2	PROVEAN	Mutation-Taster	Functional domain	ACMG classification ^b	Reference
c.50T > C p.F17S	De novo	0.007	−5.133	155	Unknown	LP	Webster et al. 2016
c.2902C > T p.R968*	De novo					P	Jansen et al. 2018
c.298_299del p.L100Ifs*13	De novo					P	Jansen et al. 2018
c.328C > A p.R110S	De novo	0.997	−5.148	110	Unknown	LP	Jansen et al. 2018
c.328C > T p.R110C	De novo	1.000	−6.841	180	Unknown	LP	Jansen et al. 2018
c.340 + 2T > C p.(?)	Unknown, not maternal					LP	Jansen et al. 2018
c.340 + 2T > C p.(?)	Unknown, not maternal					LP	Jansen et al. 2018
c.3595delG p.V1199Ter	De novo					P	Craddock et al. 2019
c.540_541insA p.G181RfsTer12	Paternal					LP	Craddock et al. 2019
c.598_599delACinsT p.T200LfsTer8	Unknown, not paternal					LP	Craddock et al. 2019
c.686C > T p.S229L	De novo	0.997	−4.195	145	WD40	LP	Craddock et al. 2019
c.774dup p.P259Tfs*9	Not known					LP	Jansen et al. 2018
c.779delT p.L260Wfs*48	De novo					P	Webster et al. 2016
c.820C > T p.Q274*	De novo					P	Jansen et al. 2018
c.860C > A p.S287Y	De novo	0.941	−1.105	144	WD40 ^c	LP	Craddock et al. 2019
c.919_923del p.I307fs	De novo					P	Jansen et al. 2018
c.1050delT p.F349fs31	Unknown, not maternal					LP	Jansen et al. 2018
c.1463 A > T p.D488V	De novo	0.99	−7.838	152	WD40 ^c	VUS	This study
c.1562A > G p.K521R	De novo	0.997	−2.513	26	unknown	LP	Craddock et al. 2019
c.1653 + 1G > A p.(?)	Unknown, not maternal					LP	Jansen et al. 2018
c.1663C > T p.Q555*	Paternal					LP	Jansen et al. 2018
c.1900C > T p.Q634*	Unknown, not maternal					LP	Jansen et al. 2018
c.2744_2747del p.K915SfsTer15	De novo					P	Craddock et al. 2019
c.2888A > G p.E963G	De novo	0.97	−6.388	98	PBR	VUS	This study ^d
c.3161delT p.L1054Ter	De novo					P	Craddock et al. 2019
c.3447T > G p.Y1149*	De novo					P	De Ligt et al. 2012
c.3447T > G p.Y1149*	De novo					P	Jansen et al. 2018
c.3571C > T p.Q1191*	De novo					P	Jansen et al. 2018
c.3782 + 3_3782 + 6delAAGT IVS32 + 3_IVS32 + 6delAAGT	Unknown, not maternal					LP	Craddock et al. 2019
c.3787C > G p.Q1263E	De novo	0.001	−1.802	29	unknown	VUS	Jansen et al. 2018
c.3801_3805del p.I1268fs	De novo					P	Jansen et al. 2018

(Continued on next page.)

Table 2. (Continued)

Variant ^a	Inheritance	PolyPhen-2	PROVEAN	Mutation-Taster	Functional domain	ACMG classification ^b	Reference
c.3892C>T p.R1298*	De novo					P	Jansen et al. 2018
c.4060A>T p.R1354*	Not known					LP	Jansen et al. 2018
c.4415_4418del p.E1472Afs*2	De novo					P	Jansen et al. 2018
c.4570delT p.S1524LfsTer22	Unknown						Craddock et al. 2019

^aScores and functional domains determined only for missense variants (highlighted in gray). Score annotations (PolyPhen-2: red = Probably damaging, orange = possibly damaging, green = benign; PROVEAN: red = deleterious, green = neutral; MutationTaster: red = disease causing).

^bAmerican College of Medical Genetics and Genomics (ACMG) classification (P = Pathogenic, LP = Likely Pathogenic, VUS = Variant of unknown significance).

^cResidue present in WD40 repeat.

^dAlso reported in an unrelated individual on DECIPHER (unknown inheritance).

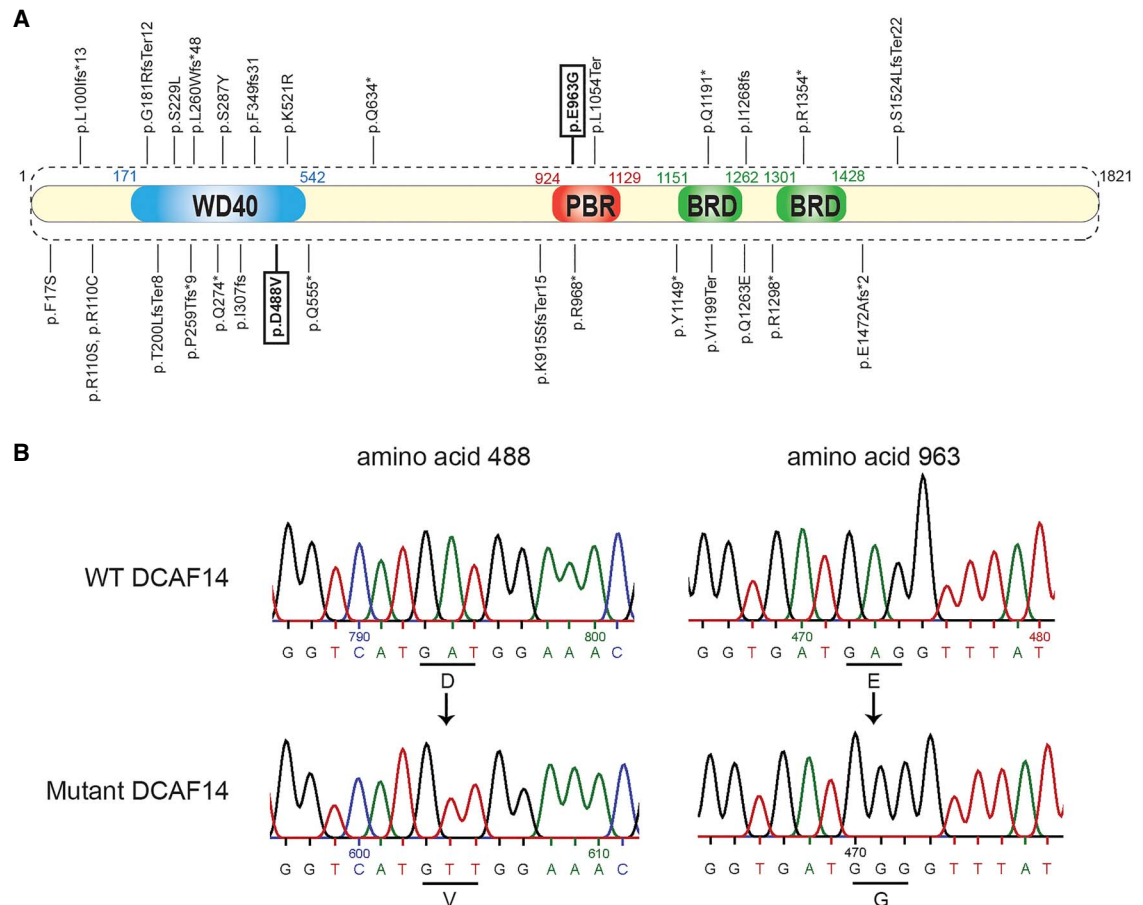


Figure 1. Domain map of DCAF14 with pathogenic variants. (A) Schematic diagram of an 1821-amino-acid-long DCAF14 with predicted functional domains. PHIP pathogenic variants listed in Table 2, excluding splice variants, are depicted. Pathogenic variants aspartic acid to valine at aa488 and glutamic acid to glycine at aa963 are highlighted. (B) DNA chromatograms to validate point mutations by site-directed mutagenesis are indicated.

She has unilateral 3-4 toe syndactyly and hypertrichosis on her forehead and lower back. Her milestones were delayed. She sat independently at 12 mo and started walking at 15–18 mo. She has history of mild hypotonia that improved with age, fine motor and gross motor delay, and excessive clumsiness and difficulty with coordination. She has neurobehavioral issues including mood swings, shyness, difficulty socializing, and reluctance to try new things. Her Vineland adaptive behavioral scale composite score was 100, communication subscore of 103, daily living skills subscore of 104, socialization subscore of 92, and motor skills subscore of 108.

Variants Exhibit Defective DNA Replication

Recent studies demonstrate critical genome maintenance functions of DCAF14 in promoting stalled fork stability by preventing replication fork collapse into double-strand breaks (Townsend et al. 2021). Furthermore, genetic analyses indicate that DCAF14 functions are CUL4-dependent because depletion of CUL4B and DDB1 mimic DCAF14 functions in replication fork protection. Because both disease variants are predicted to disrupt DCAF14 function and are present in functional domains of DCAF14, we hypothesized that both variants compromise the ability of DCAF14 to mediate replication fork stabilization (Fig. 1A). To test this hypothesis, we utilized a cDNA construct expressing epitope-tagged DCAF14 under the influence of constitutive cytomegalovirus (CMV) promoter. Full-length DCAF14 is expressed at the predicted molecular weight and rescues replication-associated phenotypes in DCAF14 knockout U2OS cell lines indicating the phenotypes are specific to DCAF14 (Townsend et al. 2021). Using site-directed mutagenesis, we generated DCAF14 cDNA constructs with missense variants either at amino acid 488 (Asp → Val) or amino acid 963 (Glu → Gly). Both mutant constructs were verified by DNA sequencing (Fig. 1B).

Next, we assessed whether replication is compromised in cells expressing pathogenic variants of DCAF14. For this purpose, we expressed the three cDNA constructs (DCAF14 wild-type, DCAF14 D488V, and DCAF14 E963G) in DCAF14 knockout U2OS cells to near-identical levels (Fig. 2A) and performed DNA fiber-labeling analyses (Fig. 2B). Cells were pulsed with thymidine analog CldU for 30 min followed by IdU for 30 min in presence of replication fork stalling agent camptothecin (CPT). CPT acts by trapping topoisomerase I-DNA bound complex resulting in replication-associated DSBs. Single replicating molecules of DNA were isolated and quantified and IdU/CldU ratios were plotted to assess changes in lengths of both IdU and CldU labels (Fig. 2B). Fiber elongation rates remain unaltered in unperturbed conditions (data not shown). Although mock transfected DCAF14 knockout cells display reduced IdU/CldU ratios in the presence of CPT, complementation with DCAF14 wild-type rescues the IdU/CldU ratios to levels observed in U2OS. In comparison, expression of both variants, D488V and E963G, fails to restore IdU/CldU ratios in the presence of CPT (Fig. 2C). A reduction in IdU/CldU ratios suggests that the newly synthesized DNA is subjected to degradation in the presence of added replication stress. To test this idea, we performed nascent strand degradation assays wherein cells are sequentially pulsed with CldU and IdU analogs for 30 min followed by exposure to replication-stalling reagent hydroxyurea (HU) for 4 h (Fig. 2D). Conditions wherein replication fork protection is intact display IdU/CldU ratios close to 1, whereas reduced IdU/CldU ratios are indicative of nascent DNA digestion. DCAF14 wild-type complemented cells restore replication fork protection consistent with previous studies (Townsend et al. 2021). In contrast, both D488V and E963G mutants fail to prevent nascent DNA digestion indicating that both disease variants disrupt DCAF14 function in protecting nascent DNA from degradation.

Impaired Genome Stability in Cells Expressing PHIP Pathogenic Variants

Perturbed DNA replication or defective function in stress response proteins undermine genome stability. We aimed to determine the consequences of impaired replication on

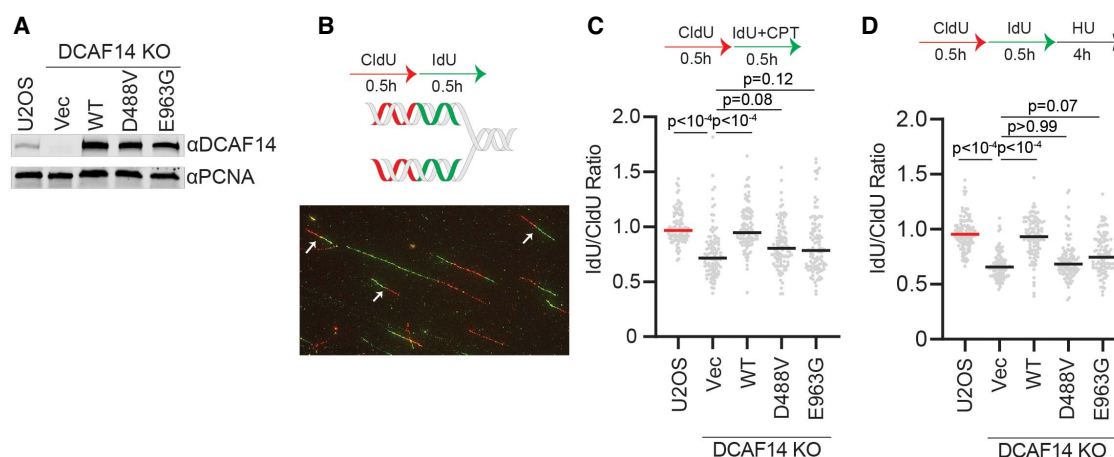


Figure 2. DCAF14 pathogenic variants exhibit defective replication fork progression. (A) An immunoblot for U2OS and DCAF14 knockout (KO) cells complemented with indicated constructs is shown. (Vec) Empty vector control, (WT) wild-type DCAF14. (B) A schematic for DNA fiber-labeling analyses. A representative immunofluorescence image of DNA fibers is shown. White arrows denote dual-labeled replication tracts utilized for quantification purposes. (C) DCAF14 KO cells expressing indicated constructs were pulse-labeled for DNA fiber analyses in the presence of CPT and harvested for immunostaining. (D) DCAF14 KO cells expressing indicated constructs were pulse-labeled as shown for nascent strand degradation assays. Graphs are representative of at least two biological replicates and include a U2OS sample as control. At least 100 fibers were analyzed. Horizontal lines depict median values. *P*-values were derived using Mann–Whitney test using 0.05 as a cutoff.

genome stability in cells expressing the CJS variants. First, we performed neutral comet assays to assess DSB formation in conditions of replication stress because failure to deal with replication stress often causes irreversible collapse into DSBs. *DCAF14* knockout cells complemented with wild-type DCAF14 are able to reverse elevated break formation in the presence of CPT, indicating break formation is DCAF14-specific (Fig. 3A,B). While the D488V variant is unable to rescue break induction, expressing the E963G variant phenocopies wild-type DCAF14 in rescuing breaks. To further corroborate this result, we analyzed chromatin-bound intensity of single-strand DNA (ssDNA)-binding protein RPA32 (Fig. 3C,D) and exposed BrdU in nondenaturing conditions (Fig. 3E,F) by quantitative imaging. Immunofluorescence studies indicate that the D488V variant fails to suppress elevated ssDNA in DCAF14 knockout cells after exposure to CPT (Fig. 3D,F). These results suggest that the aspartic acid residue at amino acid 488 plays a critical role in preventing formation of DSBs.

Underreplicated regions of the genome are transmitted to daughter cells following mitotic division and are shielded from unscheduled repair or breakage by 53BP1 bodies (Lukas et al. 2011). Thus, we sought to establish whether the replication defects in cells expressing the disease variants generate 53BP1 bodies. For this purpose, cells were treated with CPT for 24 h to induce DNA damage and released into fresh media for 3 h to allow completion of mitosis. Cells were scored for 53BP1 foci formation and stained for PCNA to differentiate replicating cells from nonreplicating cells. Exposure to CPT increases 53BP1 foci formation in PCNA-negative nuclei as expected (Fig. 3G). Whereas wild-type DCAF14 suppresses the phenotype, cells expressing either D488V or E963G display increased 53BP1 foci levels similar to mock-transfected knockout cells (Fig. 3H). Thus, cells expressing both DCAF14 disease variants fail to replicate DNA completely resulting in compromised genome integrity.

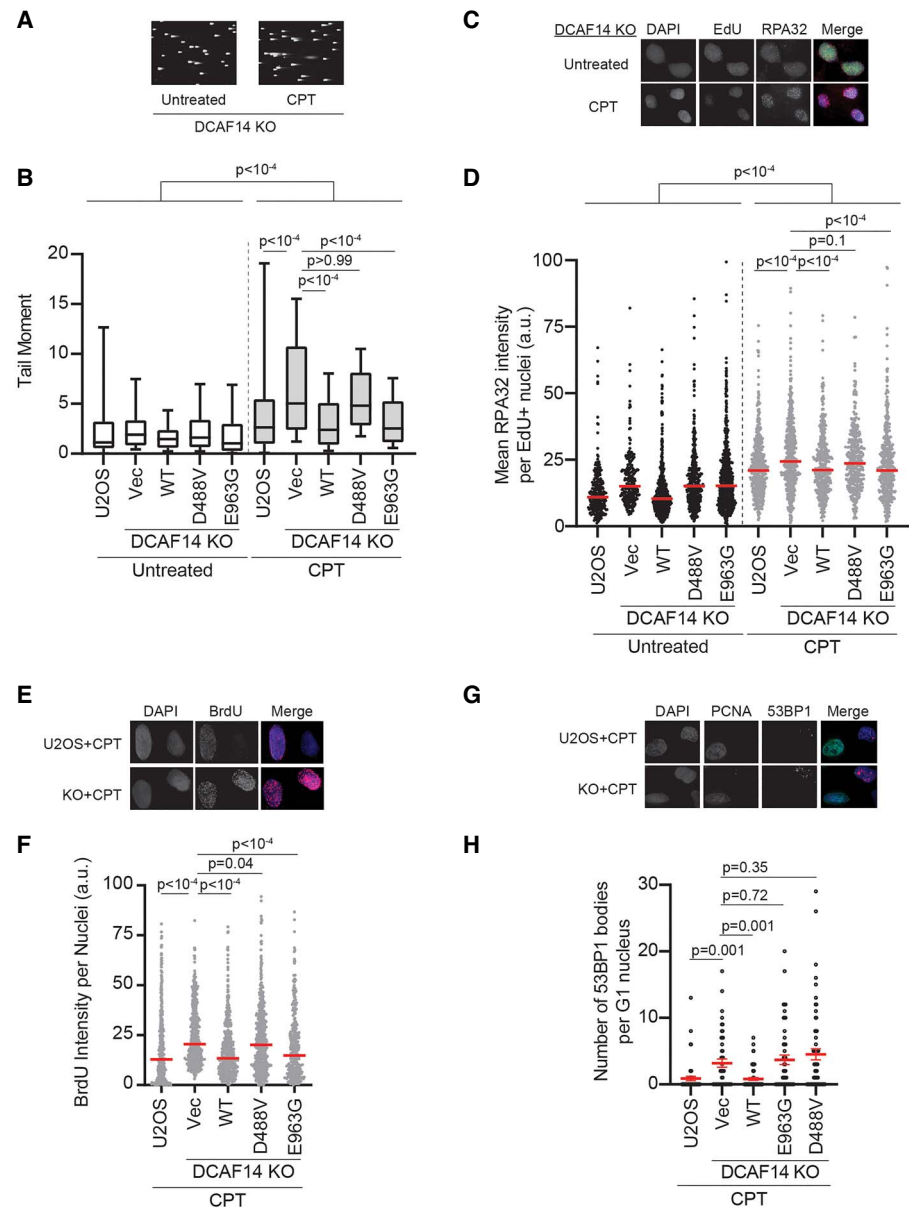


Figure 3. Increased genome instability is associated with DCAF14 pathogenic variants. (A) Representative images for a comet assay are shown. (B) Tail moments were measured for the indicated samples using neutral comet assay and graphed as box and whisker plots. (Vec) Empty vector control, (WT) wild-type DCAF14. (C) Representative images for RPA32 staining are shown. (D) Cells were left either untreated or treated with 100 nM camptothecin (CPT) for 4 h. Post-detergent extraction and fixation, cells were stained for RPA32 and intensities were analyzed by quantitative imaging. To identify replicating population, cells were pulsed with EdU for 10 min and subjected to Click chemistry to isolate S-phase nuclei. Red horizontal lines represent median values and approximately 250 nuclei were analyzed for each condition. (E) Representative images for native BrdU staining are shown. (F) Cells were pulsed with BrdU for 10 min followed by 100 nM CPT for 4 h. Nuclei were probed with anti-BrdU using nondenaturing conditions. Red horizontal lines represent median values and a minimum of 350 nuclei were analyzed for each condition. (G) Representative images for 53BP1 foci and proliferating cell nuclear antigen (PCNA) staining are shown. (H) 53BP1 foci were measured in PCNA-negative nuclei after release from 24 h of treatment with CPT. Mean \pm SEM were plotted for each sample. The graph is representative of at least two biological replicates. A minimum of 75 nuclei were assessed for each condition. *P*-values in all graphs were derived using Mann–Whitney test using 0.05 as cutoff. (a.u.) arbitrary units.

DISCUSSION

In this study, we identify and characterize two *PHIP* variants in unrelated individuals with classical features of CJS. Both variants are missense variants and occur in known functional domains of DCAF14. Using cell-based assays, we observe defective replication in both D488V- and E963G-variant-expressing cells in conditions of replication stress. Consequently, the underreplicated regions of the genome are left exposed, indicative of increased genome instability. Thus, deficiencies in mediating replication fork stability are possibly linked to the clinical presentation of CJS.

Although the E963G variant does not protect stalled forks from DSB formation, the D488V variant fails to prevent replication fork collapse, indicating both the WD40 domain and the PBR domain of DCAF14 control fork stabilization using different mechanisms. The WD40 domain of DCAF14, and other DCAFs for CRL4 complexes, functions as a bridge to recruit DCAFs to CUL4 scaffold (Jin et al. 2006). Although the substrates targeted for ubiquitination are currently unknown for CRL4^{DCAF14}, the mechanism of action for DCAF14 in DNA replication is attributed to its ability to interact with the ubiquitin ligase complex (Jang et al. 2018; Townsend et al. 2021). Indeed, loss of CRL4 subunits CUL4B and DDB1 also cause defective replication fork progression (Townsend et al. 2021). Furthermore, loss-of-function variants in *CUL4B* are also associated with overlapping symptoms of intellectual disability (Tarpey et al. 2007), implicating a critical role of the CRL4^{DCAF14} complex in genome maintenance. In this light, a recent study highlights DCAF14-mediated trivalent nucleosome recognition for CRL4 recruitment to chromatin for gene expression (Morgan et al. 2021) and further demonstrates the significance of DCAF14 in regulating several chromatin-related processes.

PHIP encodes three functional isoforms (Farhang-Fallah et al. 2000; Kato et al. 2000; Podcheko et al. 2007). Our results indicate that full-length DCAF14 is the functional isoform defective in CJS and is consistent with results highlighted in previous reports (Jansen et al. 2018; Craddock et al. 2019). The two individuals with *PHIP* variants are still relatively young (age 4-yr-old) and have typical features of CJS at this age. They are largely medically healthy and have correctable vision issues and gastrointestinal issues of constipation and reflux disease. Growth at this age is slightly below population average for height and weight. Development is delayed, and there are already behavioral features of autism or autistic-like symptoms. Notably, there is a range of adaptive behavior skills, and one individual scored at approximately the population mean in all domains yet has a typical CJS behavioral profile. This neurobehavioral profile is particularly interesting among the monogenic conditions associated with autism in that many individuals are not intellectually disabled. Importantly, genome instability has not been clinically investigated in CJS individuals, and it is unclear if the observed cellular phenotypes of fork instability might increase predisposition to certain malignancies.

Although the clinical presentation of CJS is distinct from syndromes caused by defects in either DNA replication or the replication stress response, CJS individuals have consistent features of neurocognitive and behavioral issues, dysmorphisms, and skeletal abnormalities. Biallelic variants in *ATR* are associated with facial dysmorphisms, clinodactyly, and learning disability (Mokrani-Benhelli et al. 2013). Biallelic *DONSON* variants are associated with minor skeletal abnormalities such as clinodactyly and syndactyly, coupled with mild intellectual disability (Reynolds et al. 2017). Whether these overlapping clinical features are all due in part to *PHIP* dysfunction is unknown. In contrast, clinical features of obesity are unique to CJS and are possibly linked to the replication-independent functions of *PHIP*. The tissue abundance of various *PHIP* isoforms is not known, and the distinct features could result from altered expression or activity of *PHIP* isoforms in a cell-type and tissue-specific manner.

In comparison, clinical features unique to replisome disorders highlight the role of canonical replisome components in unperturbed conditions. Although replication elongation rates remain unaltered in cells lacking DCAF14 (Townsend et al. 2021), elongation is compromised in the presence of DNA-damaging agents indicating a vital role of DCAF14 in stabilizing stalled replication forks.

In summary, the characterized CJS variants exhibit molecular phenotypes associated with defective replication fork stability and perhaps extend to previously identified individuals with either missense variants or nonsense *PHIP* variants. Future studies are essential to validate the observed genotype–phenotype relationship linking *PHIP* deficiency to genome integrity using patient-derived cell lines. Additionally, use of patient-derived cell lines will help address stress response defects in the context of *PHIP* heterozygosity. Detailed clinical characterization of CJS individuals will provide further insight into the phenotypic representation of CJS and help design effective strategies for symptom management.

METHODS

Exome Sequencing

Trio exome sequencing and Sanger sequencing validation were performed with 100-bp paired-end reads as previously described (Tanaka et al. 2015). Refer to Supplemental Table S1 for a sequencing coverage table.

Cell Culture

U2OS cell lines were cultured in DMEM media with 7.5% FBS and 5% CO₂. All transfections were performed with FuGene HD.

Synthesis of Expression Constructs

A mammalian vector expressing full-length DCAF14 was purchased from Origene (RC217114). Point mutations for the individual disease variants were introduced using QuikChange II site-directed mutagenesis kit and constructs were validated by DNA sequencing.

Synthesis of DCAF14 Knockout (KO) Cell Lines

U2OS *DCAF14* KO cell lines were generated by gene editing using CRISPR–Cas9, as previously described (Townsend et al. 2021). Briefly, U2OS cells were cotransfected with pSpCas9 (BB)-2A-Puro with guide RNA vectors targeting exon1–intron1 junction and exon 4 using FugeneHD transfection reagent. Two days post–puromycin selection, cells were harvested and seeded in 96-well dishes to isolate single cell clones. Individual clones were screened for *DCAF14* editing by PCR and immunoblotting. A single representative *DCAF14* KO clone was used in this study.

Immunofluorescence

For 53BP1 foci analyses, cells were detergent-extracted, fixed, and probed with 53BP1 and PCNA antibodies. Cells without detectable PCNA staining were scored for 53BP1 bodies. For RPA32 analysis, cells were preextracted prior to fixation to visualize chromatin-bound RPA32. After image acquisition, RPA32 intensities in EdU-positive nuclei were analyzed using Cell Profiler. For native BrdU analyses, cells were pulsed with 10 μ M BrdU for 10 min followed by 100 nM CPT treatment for 4 h. DNA fiber-labeling analyses was performed using protocols described previously (Jackson and Pombo 1998). In brief, cells were pulsed with 20 μ M CldU for 30 min followed by 100 μ M IdU for 30 min in the presence of 100 nM

CPT. For nascent strand degradation assays, cells were sequentially pulsed with CldU and IdU for 30 min followed by exposure to 4 mM HU for 4 h. After drug treatments, cells were harvested, lysed, and DNA stretched on slides using gravity. DNA was fixed with a 3:1 solution of methanol:acetic acid and slides were stored in -20°C overnight. The following day, DNA was denatured in 2.5 N HCl and blocked using goat serum with 0.1% TX-100. DNA was then costained with primary antibodies for IdU and CldU followed by staining with secondary antibodies. Images were acquired on Keyence BZ-X800 using a 60 \times oil objective. For RPA32 and BrdU quantification, images were analyzed using Cell Profiler. Hybrid cell count module on the Keyence BZ-X analyzer software was used to quantify 53BP1 foci.

Antibodies

The following antibodies were used: 53BP1 (Abcam ab21083), RPA32 (Abcam ab2175), PCNA (Santa Cruz sc-56), mouse anti-BrdU (BD Biosciences347580), rat anti-BrdU (Abcam ab6326), DCAF14 (Novus NBP2-33883), and KU70 (Abcam ab92450).

Neutral Comet Assays

Double-strand break formation was assessed using a comet assay kit from Trevigen. Tail moments were measured using Comet Score software and the data were presented as box and whisker plots.

ADDITIONAL INFORMATION

Data Deposition and Access

Variant data have been deposited in ClinVar (<https://ncbi.nlm.nih.gov/clinvar/>) and can be found under accession numbers SCV002546353 and SCV002546354.

Ethics Statement

All participants signed informed consent for a protocol approved by the Columbia University institutional review board.

Acknowledgments

We thank the subjects and their families for participation in this study.

Author Contributions

N.T.C., C.H., and H.D. designed the experimental strategy, performed experiment, and interpreted data. W.K.C. provided clinical data related to the subjects. W.K.C. and H.D. compiled and wrote the manuscript with input from other authors.

Funding

H.D. received support from National Institutes of Health (NIH) grant 1R35GM137800. W.K.C. received support from the Simons Foundation Autism Research Institute (SFARI) and the JPB foundation.

REFERENCES

Bellelli R, Boulton SJ. 2021. Spotlight on the replisome: aetiology of DNA replication-associated genetic diseases. *Trends Genet* **37**: 317–336. doi:10.1016/j.tig.2020.09.008

Competing Interest Statement

The authors have declared no competing interest.

Received April 14, 2022;
accepted in revised form
June 27, 2022.

- Boerkoel CF, Takashima H, John J, Yan J, Stankiewicz P, Rosenbarker L, André JL, Bogdanovic R, Burguet A, Cockfield S, et al. 2002. Mutant chromatin remodeling protein SMARCAL1 causes Schimke immuno-osseous dysplasia. *Nat Genet* **30**: 215–220. doi:10.1038/ng821
- Craddock KE, Okur V, Wilson A, Gerkes EH, Ramsey K, Heeley JM, Juusola J, Vitobello A, Dupeyron MB, Faivre L, et al. 2019. Clinical and genetic characterization of individuals with predicted deleterious PHIP variants. *Cold Spring Harb Mol Case Stud* **5**: a004200. doi:10.1101/mcs.a004200
- Cunniff C, Bassetti JA, Ellis NA. 2017. Bloom's syndrome: clinical spectrum, molecular pathogenesis, and cancer predisposition. *Mol Syndromol* **8**: 4–23. doi:10.1159/000452082
- de Ligt J, Willemsen MH, van Bon BW, Kleefstra T, Yntema HG, Kroes T, Vulto-van Silfhout AT, Koolen DA, de Vries P, Gilissen C, et al. 2012. Diagnostic exome sequencing in persons with severe intellectual disability. *N Engl J Med* **367**: 1921–1929. doi:10.1056/NEJMoa1206524
- De Semir D, Nosrati M, Bezrookove V, Dar AA, Federman S, Bienvenu G, Venna S, Rangel J, Climent J, Meyer Tamgüney TM, et al. 2012. Pleckstrin homology domain-interacting protein (PHIP) as a marker and mediator of melanoma metastasis. *Proc Natl Acad Sci* **109**: 7067–7072. doi:10.1073/pnas.1119949109
- Farhang-Fallah J, Yin X, Trentin G, Cheng AM, Rozakis-Adcock M. 2000. Cloning and characterization of PHIP, a novel insulin receptor substrate-1 pleckstrin homology domain interacting protein. *J Biol Chem* **275**: 40492–40497. doi:10.1074/jbc.C000611200
- Fujisawa T, Filippakopoulos P. 2017. Functions of bromodomain-containing proteins and their roles in homeostasis and cancer. *Nat Rev Mol Cell Biol* **18**: 246–262. doi:10.1038/nrm.2016.143
- Jackson DA, Pombo A. 1998. Replicon clusters are stable units of chromosome structure: evidence that nuclear organization contributes to the efficient activation and propagation of S phase in human cells. *J Cell Biol* **140**: 1285–1295. doi:10.1083/jcb.140.6.1285
- Jang SM, Zhang Y, Utani K, Fu H, Redon CE, Marks AB, Smith OK, Redmond CJ, Baris AM, Tulchinsky DA, et al. 2018. The replication initiation determinant protein (ReplID) modulates replication by recruiting CUL4 to chromatin. *Nat Commun* **9**: 2782. doi:10.1038/s41467-018-05177-6
- Jang SM, Nathans JF, Fu H, Redon CE, Jenkins LM, Thakur BL, Pongor LS, Baris AM, Gross JM, O'Neill MJ, et al. 2020. The ReplID-CRL4 ubiquitin ligase complex regulates metaphase to anaphase transition via BUB3 degradation. *Nat Commun* **11**: 24. doi:10.1038/s41467-019-13808-9
- Jansen S, Hoischen A, Coe BP, Carvill GL, Van Esch H, Bosch DGM, Andersen UA, Baker C, Bauters M, Bernier RA, et al. 2018. A genotype-first approach identifies an intellectual disability-overweight syndrome caused by PHIP haploinsufficiency. *Eur J Hum Genet* **26**: 54–63. doi:10.1038/s41431-017-0039-5
- Jin J, Arias EE, Chen J, Harper JW, Walter JC. 2006. A family of diverse Cul4-Ddb1-interacting proteins includes Cdt2, which is required for S phase destruction of the replication factor Cdt1. *Mol Cell* **23**: 709–721. doi:10.1016/j.molcel.2006.08.010
- Kato H, Chen S, Kiyama H, Ikeda K, Kimura N, Nakashima K, Taga T. 2000. Identification of a novel WD repeat-containing gene predominantly expressed in developing and regenerating neurons. *J Biochem* **128**: 923–932. doi:10.1093/oxfordjournals.jbchem.a022843
- Ladha S. 2011. Of ORC and forks: the identification of mutations implicated in Meier-Gorlin syndrome. *Clin Genet* **80**: 506–507. doi:10.1111/j.1399-0004.2011.01779.x
- Lukas C, Savic V, Bekker-Jensen S, Doil C, Neumann B, Sølvhøj Pedersen R, Grøfte M, Chan KL, Hickson ID, Bartek J, et al. 2011. 53BP1 nuclear bodies form around DNA lesions generated by mitotic transmission of chromosomes under replication stress. *Nat Cell Biol* **13**: 243. doi:10.1038/ncb2201
- Mokrani-Benhelli H, Gaillard L, Biasutto P, Le Guen T, Touzot F, Vasquez N, Komatsu J, Conseiller E, Picard C, Gluckman E, et al. 2013. Primary microcephaly, impaired DNA replication, and genomic instability caused by compound heterozygous ATR mutations. *Hum Mutat* **34**: 374–384. doi:10.1002/humu.22245
- Morgan MAJ, Popova IK, Vaidya A, Burg JM, Marunde MR, Rendleman EJ, Dumar ZJ, Watson R, Meiners MJ, Howard SA, et al. 2021. A trivalent nucleosome interaction by PHIP/BRWD2 is disrupted in neurodevelopmental disorders and cancer. *Genes Dev* **35**: 1642–1656. doi:10.1101/gad.348766.121
- O'Driscoll M, Ruiz-Perez VL, Woods CG, Jeggo PA, Goodship JA. 2003. A splicing mutation affecting expression of ataxia-telangiectasia and Rad3-related protein (ATR) results in Seckel syndrome. *Nat Genet* **33**: 497–501. doi:10.1038/ng1129
- Ogi T, Walker S, Stiff T, Hobson E, Limsirichaikul S, Carpenter G, Prescott K, Suri M, Byrd PJ, Matsuse M, et al. 2012. Identification of the first ATRIP-deficient patient and novel mutations in ATR define a clinical spectrum for ATR-ATRIP Seckel syndrome. *PLoS Genet* **8**: e1002945. doi:10.1371/journal.pgen.1002945
- Oshima J, Sidorova JM, Monnat RJ Jr. 2017. Werner syndrome: clinical features, pathogenesis and potential therapeutic interventions. *Ageing Res Rev* **33**: 105–114. doi:10.1016/j.arr.2016.03.002
- Podcheko A, Northcott P, Bikopoulos G, Lee A, Bommarreddi SR, Kushner JA, Farhang-Fallah J, Rozakis-Adcock M. 2007. Identification of a WD40 repeat-containing isoform of PHIP as a novel regulator of beta-cell growth and survival. *Mol Cell Biol* **27**: 6484–6496. doi:10.1128/MCB.02409-06

- Reynolds JJ, Bicknell LS, Carroll P, Higgs MR, Shaheen R, Murray JE, Papadopoulos DK, Leitch A, Murina O, Tarnauskaitė Z, et al. 2017. Mutations in DONSON disrupt replication fork stability and cause microcephalic dwarfism. *Nat Genet* **49**: 537–549. doi:10.1038/ng.3790
- Saldivar JC, Cortez D, Cimprich KA. 2017. The essential kinase ATR: ensuring faithful duplication of a challenging genome. *Nat Rev Mol Cell Biol* **18**: 622–636. doi:10.1038/nrm.2017.67
- Tanaka AJ, Cho MT, Millan F, Juusola J, Retterer K, Joshi C, Niyazov D, Garnica A, Gratz E, Deardorff M, et al. 2015. Mutations in SPATA5 are associated with microcephaly, intellectual disability, seizures, and hearing loss. *Am J Hum Genet* **97**: 457–464. doi:10.1016/j.ajhg.2015.07.014
- Tarpey PS, Raymond FL, O'Meara S, Edkins S, Teague J, Butler A, Dicks E, Stevens C, Tofts C, Avis T, et al. 2007. Mutations in CUL4B, which encodes a ubiquitin E3 ligase subunit, cause an X-linked mental retardation syndrome associated with aggressive outbursts, seizures, relative macrocephaly, central obesity, hypogonadism, pes cavus, and tremor. *Am J Hum Genet* **80**: 345–352. doi:10.1086/511134
- Townsend A, Lora G, Engel J, Tirado-Class N, Dungrawala H. 2021. DCAF14 promotes stalled fork stability to maintain genome integrity. *Cell Rep* **34**: 108669. doi:10.1016/j.celrep.2020.108669
- Webster E, Cho MT, Alexander N, Desai S, Naidu S, Bekheirnia MR, Lewis A, Retterer K, Juusola J, Chung WK. 2016. De novo PHIP-predicted deleterious variants are associated with developmental delay, intellectual disability, obesity, and dysmorphic features. *Cold Spring Harb Mol Case Stud* **2**: a001172. doi:10.1101/mcs.a001172
- Zeman MK, Cimprich KA. 2014. Causes and consequences of replication stress. *Nat Cell Biol* **16**: 2–9. doi:10.1038/ncb2897



***PHIP* variants associated with Chung–Jansen syndrome disrupt replication fork stability and genome integrity**

Neysha Tirado-Class, Caitlin Hathaway, Wendy K. Chung, et al.

Cold Spring Harb Mol Case Stud 2022, **8**: a006212 originally published online July 21, 2022
Access the most recent version at doi:[10.1101/mcs.a006212](https://doi.org/10.1101/mcs.a006212)

Supplementary Material	http://molecularcasestudies.cshlp.org/content/suppl/2022/08/03/mcs.a006212.DC1
References	This article cites 29 articles, 7 of which can be accessed free at: http://molecularcasestudies.cshlp.org/content/8/5/a006212.full.html#ref-list-1
License	This article is distributed under the terms of the Creative Commons Attribution-NonCommercial License, which permits reuse and redistribution, except for commercial purposes, provided that the original author and source are credited.
Email Alerting Service	Receive free email alerts when new articles cite this article - sign up in the box at the top right corner of the article or click here .
